Advanced Engineering Informatics 51 (2022) 101536

Contents lists available at ScienceDirect

Advanced Engineering Informatics

journal homepage: www.elsevier.com/locate/aei

Full length article

Solving the vehicle routing problem with drone for delivery services using an ant colony optimization algorithm

Shan-Huen Huang [a], Ying-Hua Huang [b], Carola A. Blazquez [c,*], Chia-Yi Chen [a]

[a] Department of Logistics Management, National Kaohsiung University of Science and Technology, No. 1, University Rd., Yanchao Dist., Kaohsiung City 824, Taiwan
[b] Department of Civil and Construction Engineering, National Yunlin University of Science and Technology, 123 University Road, Sec. 3, Douliu, Yunlin 64002, Taiwan
[c] Department of Engineering Sciences, Universidad Andres Bello, Quillota 980, Viña del Mar, Chile

ARTICLE INFO

Keywords:
Unmanned aerial vehicle
Urban delivery
Heuristic
Vehicle routing problem
Optimization

ABSTRACT

E-commerce and logistics companies are facing important challenges to satisfy the rapid growth of customer demands. Unmanned aerial vehicles such as drones are an emerging technology that are very useful to cope with rising customer expectations of fast, flexible, and reliable delivery services. Drones work in tandem with trucks to perform parcel delivery, which have proven to reduce costs, CO2 emissions, and delivery times. This research proposes a mixed integer programming formulation to address the Vehicle Routing Problem with Drone (VRPD) by assigning customers to drone-truck pairs, determining the number of dispatching drone-truck units, and obtaining optimal service routes while the fixed and travel costs of both vehicles are minimized. Given the NP-hard nature of the VRPD, an ant colony optimization (ACO) algorithm is elaborated to solve this problem. Two novel methods are proposed to investigate the efficiency of the drone-truck combination by allowing the drones to perform additional delivery services to only one feasible customer and also multiple feasible customers while the truck waits at a customer location. Experimental results show that the proposed ACO algorithm can effectively solve the VRDP for different size instances and different customer location distributions, and is successful in providing timely solutions for small test instances within 1% of the optimal solutions. Finally, experimentation also reveals that the ACO algorithm outperforms the classical VRP by obtaining cost-savings of over 30% for large instances.

1. Introduction

In the last few decades, the logistics industry has undergone a significant and rapid growth worldwide, generating many jobs and considerable annual revenues [1]. Amid this growth, logistics companies are facing important challenges to satisfy increasing customer demands in an efficient and effective manner. New technologies have been deployed in logistics strategies to provide intelligent solutions to cope with the rising customer expectations of delivering fast, flexible, and reliable services. These technologies have shown to lower costs and reduce delivery times while improving customer satisfaction [2,3].

Unmanned aerial vehicles such as drones are an emerging technology that are very useful in overcoming delivery problems in disaster relief operations [4], healthcare [5], and logistics and retail industries [6]. Drones conform a novel dispatching method that provides a fast and easy delivery service [7]. As opposed to the delivery trucks, drones have the advantage of not being restricted to the road network or confront traffic congestion that may result in dispatching delays. However, drones have a limited capacity of one or few packages and a limited flight range requiring frequent recharging or replacement of batteries for continuing their flight operations [8]. Therefore, an adequate synchronization between of trucks and drones in the delivery process is required while yielding low costs and high efficiency.

The Vehicle Routing Problem (VRP) is one of the essential issues in logistics management. Conventionally, the VRP obtains the dispatching plan for trucks located at the depot to serve customers. Different VRP variants exist in the literature to accommodate different conditions and requirements such as the pickup and delivery VRP [9], heterogeneous fleet VRP [10], multi-depot VRP [11,12], among others. In recent years, auxiliary vehicles (e.g., motorcycle, trailer, small van, or drone) have been employed to assist primary vehicles (e.g., large trucks) in servicing customers, particularly when encountering poor parking conditions or

* Corresponding author.
E-mail addresses: shanhuen@nkust.edu.tw (S.-H. Huang), huangyh@yuntech.edu.tw (Y.-H. Huang), cblazquez@unab.cl (C.A. Blazquez), f108115110@nkust.edu.tw (C.-Y. Chen).

https://doi.org/10.1016/j.aei.2022.101536
Received 1 October 2021; Received in revised form 10 December 2021; Accepted 17 January 2022
Available online 2 February 2022

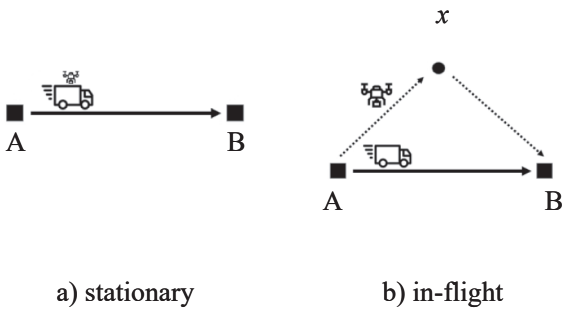

Fig. 1. Example of drone actions.

scarce vehicle accessibility. This type of vehicle dispatching problem, namely Feeder VRP (FVRP), is more complex than conventional VRP because schedules and routes of at least two vehicles need to be planned simultaneously. Some studies on FVRP are found in the literature [13,14,2].

The VRP with drone (VRPD) is an emerging topic for delivering small packages due to cost-savings, reduced CO2 emissions, and lower delivery times [15]. VRPD is a specific type of FVRP since drones are employed as auxiliary vehicles that concurrently serve customers with trucks. Drones meet with trucks at customer locations (i.e., joints) for reloading and battery recharging or replacement. Subsequently, the drones meet with trucks at other joints until the delivery service is completed. The use of drones as auxiliary vehicles is probably the most cost-effective when assisting conveyance since they are faster and more economical than the trucks [16,17], and thus, drones form an emerging and promising technology to be deployed in the near future.

This study introduces a MIP formulation of the VRPD and solves this problem using a proposed ACO algorithm for different benchmark scenarios. Small instances are solved to optimality and then compared with the ACO algorithm results. Additionally, ACO is used to solve the VRPD for instances up to 200 customers that are clustered (C), random (R), and random-clustered (RC). We present and implement two novel drone service modes, in which, in addition to synchronizing trucks and drones to perform a collaborative delivery process in the VRPD, the drones also may serve customers while the trucks halt at customer locations.

The remainder of this study is structured as follows: Section 2 presents a literature review. Section 3 describes the problem, illustrates the typical drone distribution mode, formulates the mathematical model for the VRPD, and presents the two novel drone service modes. Section 4 describes the benchmark and the proposed solution approach. Section 5 presents the computational results and a comparison with the traditional VRP. Finally, Section 6 presents the conclusions and future research.

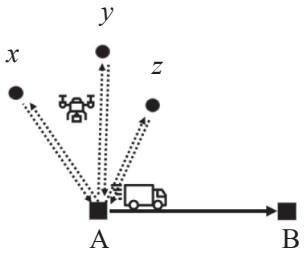

Fig. 3. Additional flying action of the drone (FS^{+} mode).

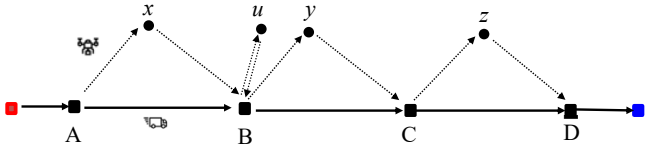

Fig. 4. Example of FS^{+1} method.

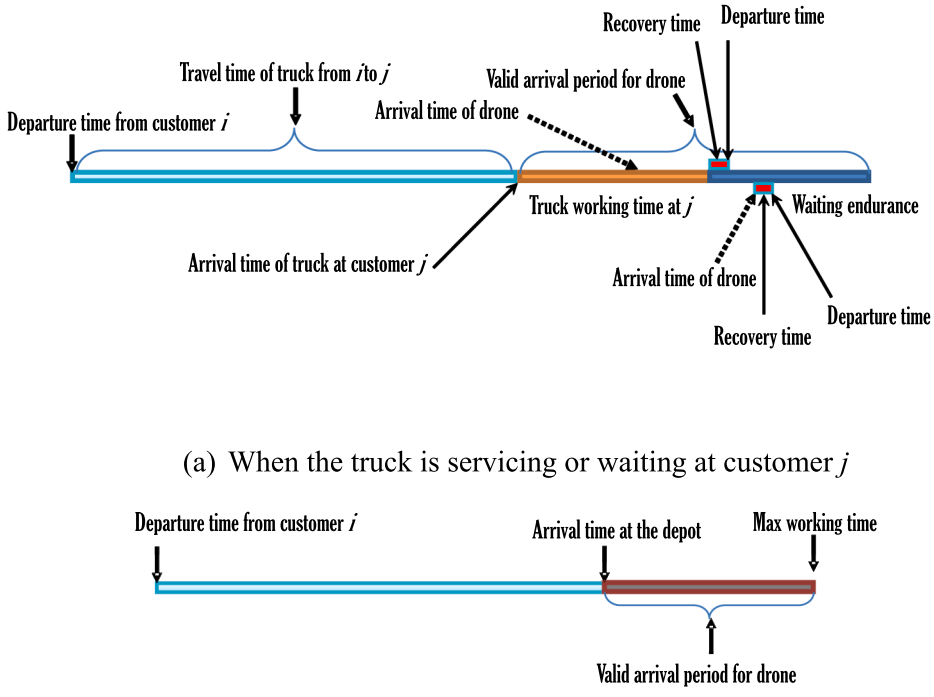

Fig. 2. Dronés arrival times.

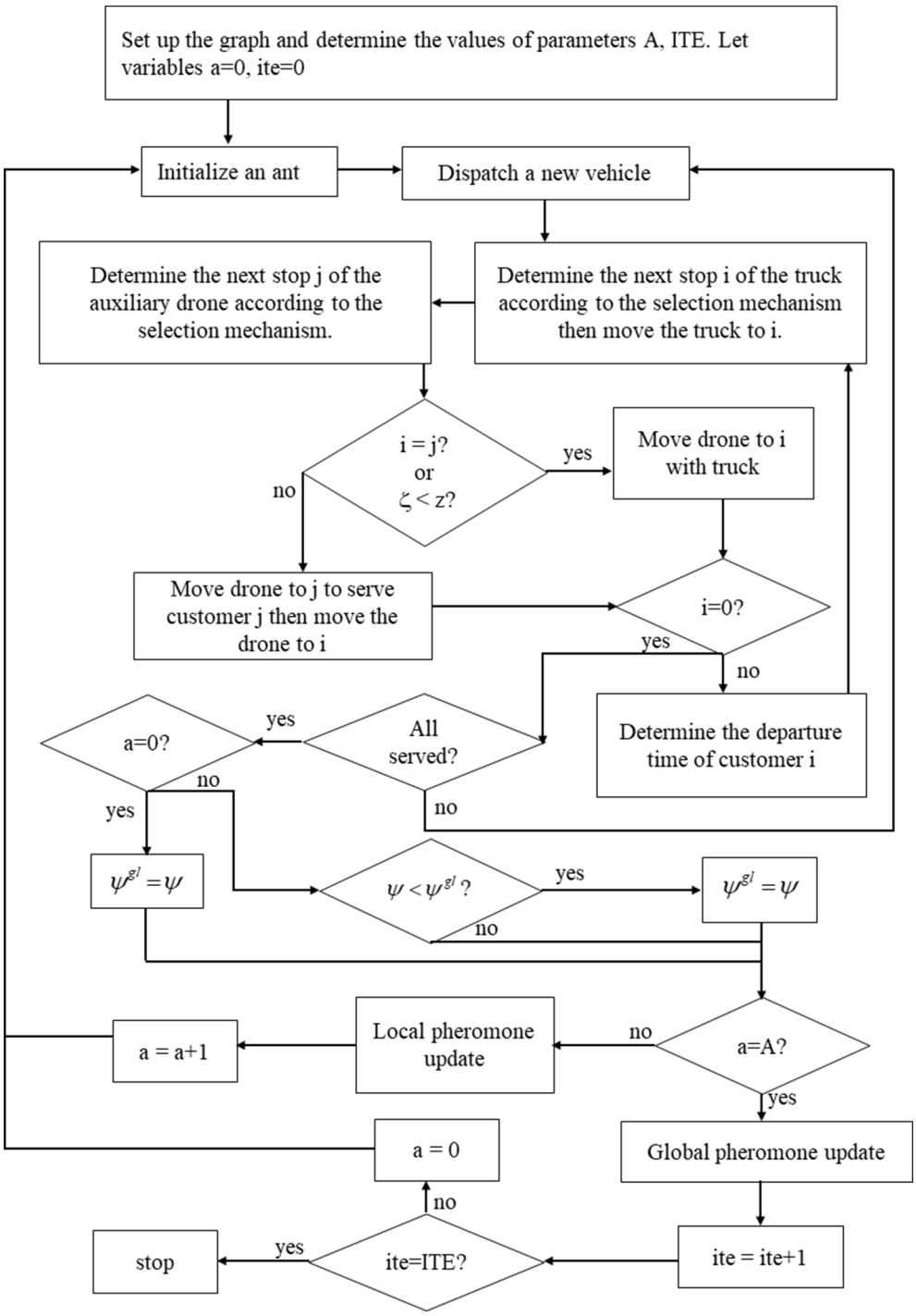

Fig. 5. Flowchart of the ACO solving process.

2. Literature review

VRPD and its variants have been widely investigated in recent years and are currently an ongoing research topic [18–22,15,23,24]. For example, Poikonen et al. [19] solved the VRPD by minimizing the total time for delivering all customer packages using a fleet of trucks with their respective number of drones. Kitjacharoenchai and Lee [20] proposed a model that synchronizes the trucks and multiple drones for parcel delivery while considering truck and drone capacities and minimizing arrival time of both vehicles at the depot. As opposed to the aforementioned studies, our study consists of drone-truck pairs that perform collaborative work by following optimal delivery routes while minimizing fixed and travel costs of the vehicles. Euchi and Sadok [23] formulated a MILP model that takes into account dependent and independent parcel deliveries, in which a truck-drone pair work in tandem and also work separately from each other to service customers. Similarly to these authors‘ work, we propose two novel service modes to allow drones to serve customers as a truck is in motion or idling at customer locations.

In other studies, MIP models are formulated so that drones may take off from a truck and subsequently land on a different truck after serving their assigned customers [21,15]. Guerriero et al. [18] presented a multi-objective formulation for the VRPD with soft time windows, while considering simultaneously the traveled distances, customer

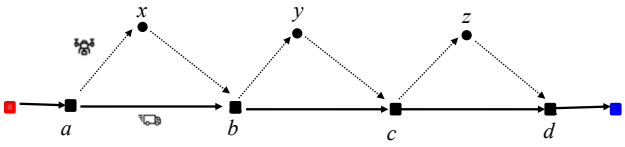

a) Visit sequence before applying 2-opt method

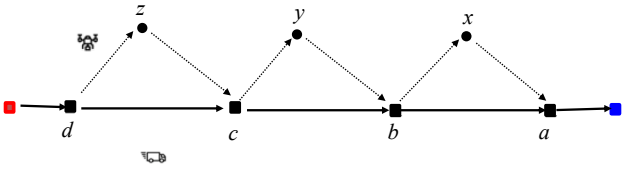

b) Visit sequence after applying 2-opt method

Fig. 6. Illustration of 2-opt on a truck-drone route.

satisfaction, and number of drones. Chung et al. [22] and Viloria et al. [24] provide for more details on the modeling of the VRPD.

Due to the NP-hard nature of VRP and its variants (e.g., VRPD), various heuristic and metaheuristics approaches have been developed to solve this problem [25–33,15,34,35,23]. Studies have employed heuristic approaches such as hybrid Clarke and Wright heuristic algorithm [27], optimization-driven progressive algorithm [28], and heuristic two-phase strategy embedded in a multi-start framework to solve different variants of the VRPD [34]. Other studies solved this problem for different benchmark instances using metaheuristics such as adaptive large neighborhood search metaheuristic [29], and hybrid genetic algorithm [23]. Combinations of metaheuristics have also been developed for solving the problem such as the route construction and large neighborhood search [33], Tabu Search algorithm and Analytical Hierarchy Process [36], and variable neighborhood search and Tabu search [35]. In addition, Schermer et al. [30] proposed a matheuristic approach that uses a heuristic framework with an embedded mathematical programming to solve the problem with large instances. Finally, studies have proposed nature-inspired metaheuristics such as simulated annealing heuristics [25], improved artificial bee colony algorithm [31,32], and Swarm intelligence metaheuristics [26].

Ant Colony Optimization (ACO) is a heuristic algorithm that has been widely used to provide good solutions to the VRP and its variants within a reasonable period of time. Experimental results suggest that the ACO performance is competitive with other techniques used to generate solutions to the VRP. Unlike some algorithms that need to tackle infeasible solutions frequently, ACO can ensure the feasibility of the generated solutions in an efficient and rapid manner, meaning that ACO may ensure the search within the solution domain [37–39,2,40]. Studies have used variants of ACO metaheuristic approaches to address the VRP with fleets that comprise solely drones [41–45]. In recent years, studies have utilized ACO to solve the traveling salesman problem with drone, TSPD [46–49], but few studies are found in the literature that have addressed VRPD using ACO [50,51], as in this research. For example, Das et al. [50] formulated a bi-objective MIP model of the VRPD that minimized travel costs and maximizes customer service and solved the problem using a collaborative pareto ACO algorithm. In another study, Gu et al. [51] presented two advanced ACO with variable visibility and multilevel feedback pheromones to solve the VRPD considering instant delivery operations.

3. Problem description

In this study, the VRPD is a vehicle routing problem, where a drone is utilized as an auxiliary vehicle to a truck to help expedite the delivery process of small packages. The truck and drone depart from the depot, serve customers, and subsequently return to the depot. Both vehicles may depart or return to the depot in tandem or separately. The drone has two actions during the delivery process: i) Stationary: a drone travels on a truck from node A to node B (saving battery power) and has no mission assigned to serve any customers during this action, as shown in Fig. 1a); ii) In-flight: a drone has a mission to serve a single customer × while a truck travels from node A to node B, as depicted in Fig. 1b). These types of drone movements are known as the Flying Sidekick (FS) mode.

The assumptions are the following.

1. All vehicles depart their routes at the depot and end their routes at the depot before the work shift terminates.
2. All customer demands consist of the same type of cargo and must be served during working hours within one day.
3. A drone tour is only allowed to start and end at customer nodes.
4. Every customer (node) may be served once by either a truck or a drone and every node is a possible joint.
5. Only the truck has a capacity constraint and each drone can only deliver one package at a time.

Table 1
Comparison results between ACO and optimization model for the VRPD (FS mode).

Instances	NC	Model Results				ACO Results			△%Total Cost
		CPU (s)	SF	Total Cost	GAP Model	CPU (s)	SF	Total Cost	
C01	5	0.33	1	4873.17	0.02%	0.19	1	4873.18	0.00%
	10	140.59	1	4938.54	0.02%	0.48	1	4938.84	0.01%
	15	7200	1	4962.89	1.12%	0.87	1	4963.87	0.02%
	20	7200	1	4978.56	1.61%	1.49	1	4980.38	0.04%
	25	7200	1	4996.33	1.97%	2.2	1	4998.24	0.04%
	30	7200	1	5116.10	3.59%	4.08	1	5135.20	0.37%
R01	5	0.45	1	5030.66	0.10%	0.18	1	5030.66	0.00%
	10	303.05	1	5192.96	0.01%	0.54	1	5192.96	0.00%
	15	7200	1	5261.23	3.56%	0.75	1	5265.69	0.08%
	20	7200	1	5311.98	3.84%	1.44	1	5317.82	0.11%
	25	7200	1	5394.35	5.55%	1.81	1	5419.35	0.46%
	30	7200	1	5440.49	7.45%	3.69	1	5473.95	0.61%
RC01	5	1.03	1	5249.82	0.03%	0.2	1	5249.82	0.00%
	10	126.86	1	5145.35	0.04%	0.48	1	5145.35	0.00%
	15	7200	1	5226.11	2.56%	0.88	1	5226.11	0.00%
	20	7200	1	5189.7	2.63%	1.57	1	5203.46	0.27%
	25	7200	1	5228.99	3.53%	2.04	1	5281.89	1.01%
	30	7200	1	5270.3	5.10%	3.91	1	5325.76	1.05%

Note: NC: number of customers; CPU: CPU time (s); SF: number of sub-fleets; Total: total cost; GAP Model: Integrality GAP; Δ% Total Cost: ratio between the ACO and model cost difference and the model cost.

Table 2
Best output results for the benchmark using the ACO (FS mode).

Instances		Parameters			SF	CPU (s)	Distances		Costs			
	NC	α	β	z			TTD	DTD	TFC	TTC	DTC	Total Cost
C01	50	2	8	0	1	11.09	121.91	221.29	4796	402.30	73.03	5271.32
C02	50	4	9	0.05	2*	8.51	156.64	353.66	5232	516.91	116.71	5865.63
C03	50	9	6	0.2	2	7.62	180.64	251.80	9592	596.11	83.09	10271.19
C04	50	9	6	0	2*	8.68	149.55	279.05	5232	493.52	92.09	5817.60
C05	100	9	8	0	2	29.82	158.47	328.33	9592	522.95	108.35	10223.31
C06	100	7	8	0	2	32.66	175.19	352.00	9592	578.13	116.16	10286.30
C07	100	3	7	0.15	2	29.31	216.88	374.66	9592	715.70	123.64	10431.35
C08	100	9	5	0	2	26.22	214.46	400.73	9592	707.72	132.24	10431.97
C09	200	2	9	0.05	4	138.66	362.31	682.71	19,184	1195.62	225.29	20604.90
C10	200	4	9	0	4	126.92	317.99	542.51	19,184	1049.37	179.03	20412.40
C11	200	3	8	0.25	4	137.26	325.78	486.29	19,184	1075.07	160.48	20419.55
C12	200	7	8	0.15	4	133.80	357.47	534.03	19,184	1179.65	176.23	20539.88
R01	50	10	10	0.1	2	9.3	231.56	355.86	9592	764.15	117.43	10473.60
R02	50	5	7	0.25	2	9.31	200.68	374.52	9592	662.24	123.59	10377.84
R03	50	5	7	0.1	2	8.25	205.54	399.46	9592	678.28	131.82	10402.10
R04	50	3	6	0.1	2	7.33	220.66	361.61	9592	728.18	119.33	10439.50
R05	100	6	8	0.3	3	30.58	330.13	552.75	14,388	1089.43	182.41	15659.83
R06	100	6	6	0.1	3	28.06	326.16	700.00	14,388	1076.33	231.00	15695.33
R07	100	3	8	0	3	31.41	332.95	655.63	14,388	1098.74	216.36	15703.10
R08	100	6	8	0.25	3	32.44	329.27	503.72	14,388	1086.59	166.23	15640.82
R09	200	2	10	0	4	137.42	482.82	936.31	19,184	1593.31	308.98	21086.26
R10	200	5	9	0	4	139.03	485.60	954.93	19,184	1602.48	315.13	21101.61
R11	200	1	10	0	4	137.35	459.95	922.34	19,184	1517.84	304.37	21006.22
R12	200	7	8	0	4	137.76	480.24	941.83	19,184	1584.79	310.80	21079.60
RC01	50	2	6	0.05	2	7.89	181.76	360.71	9592	599.81	119.03	10310.85
RC02	50	8	9	0.15	2	9.47	215.94	346.96	9592	712.60	114.50	10419.11
RC03	50	10	8	0.3	2	8.79	179.97	338.89	9592	593.90	111.83	10297.75
RC04	50	10	10	0	2*	8.94	153.39	297.89	5232	506.19	98.30	5836.50
RC05	100	7	8	0	3	31.63	261.95	508.14	14,388	864.44	167.69	15420.14
RC06	100	9	10	0.05	2	31.19	291.66	527.97	9592	962.48	174.23	10728.72
RC07	100	9	9	0.05	2	29.93	262.90	588.30	9592	867.57	194.14	10653.71
RC08	100	1	10	0.15	3	31.24	275.81	458.56	14,388	910.17	151.32	15449.51
RC09	200	1	10	0	4	138.26	463.83	839.87	19,184	1530.64	277.16	20991.80
RC10	200	5	10	0.1	4	141.89	445.06	720.07	19,184	1468.70	237.62	20890.32
RC11	200	2	9	0	4	136.42	420.40	804.36	19,184	1387.32	265.44	20836.77
RC12	200	8	10	0	4	138.95	423.00	790.61	19,184	1395.90	260.90	20840.82

Note: *: one drone is dispatched as 2nd sub-fleet; NC: number of customers; SF: number of sub-fleets; CPU: CPU time (s);α: pheromone intensity weight in Eq. (34);β: pheromone visibility weight in Eq. (34); z: parameter for determining a drone's action; TTD: truck travel distance; DTD: drone travel distance; TFC: total fixed costs; TTC: truck travel costs; DTC: drone travel costs.

6. A single drone is accompanied by a specific truck, and one truck can only reload its assigned drone.
7. There is no travel cost for the drone while it travels on the truck.
8. The drone must travel to the truck's next node as soon as it completes a mission. The truck must be located at the next node before the drone's arrival.
9. A recovery time is required for the drone after meeting with the truck to get ready for the next mission.
10. The reloading time of the drone is negligible since only one package is loaded.
11. The total costs consist of fixed route and travel costs.

According to assumption 8, the drone must meet with the truck at a customer location within a specific period. Fig. 2a) illustrates that the drone must arrive at the joint (i.e., customer j) either during the truck working time or the waiting endurance. If the drone arrives at the joint during the truck working time, then the drone must wait until the truck completes its service. Thus, the truck and drone's departure time for the next node will correspond to the truck's service time plus the drone's recovery time. If the drone arrives at the joint during the truck's waiting endurance, then the drone may be dispatched immediately after the dronés recovery time. Thus, the departure time of the truck and drone for the next node will be the drone's arrival time plus the dronés recovery time. Fig. 2b) shows when the truck returns to the depot.

The model is formulated with the following sets, parameters, and decision variables to solve the VRPD.

Model parameters:	
O	depot
c_{ij}^T	travel cost of truck T between node i and node j
c_{ij}^D	travel cost of drone D between node i and node j
f^T	fixed cost for truck T
f^D	fixed cost for drone D
q_i	customer demand of node i
Q	truck capacity
t_{ij}^T	travel time of truck T between node i and node j
t_{ij}^D	travel time of drone D between node i and node j
s_i^T	customer service time of truck T at node i
s_i^D	customer service time of drone D at node i
r	recovery time of a drone
F	maximum flying time of a drone
W	maximum waiting time of truck at a joint
T	maximum shift time
Indices:	
i, j, l	indexes for nodes
k	index for vehicle (truck or drone)
Sets:	
N	set of nodes (includes the depot)
I	set of customers
K	set of vehicles belonging to a sub-fleet (i.e., truck-drone pair)
S	subset of I
Decision variables:	
x_{ijk}^T	binary variable, = 1 if truck k travels from node i to node j, 0 otherwise

(*continued on next page*)

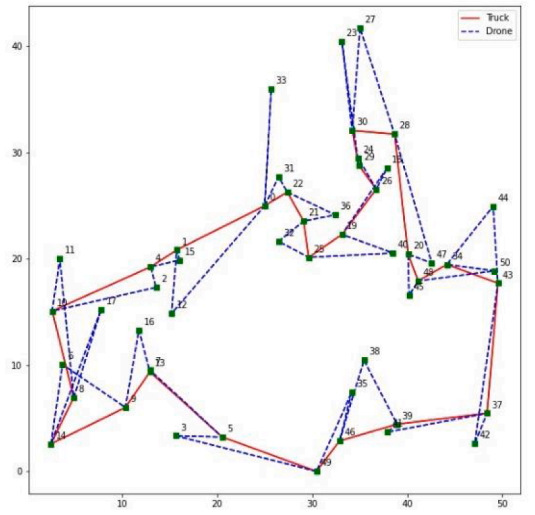

a) Instance C02

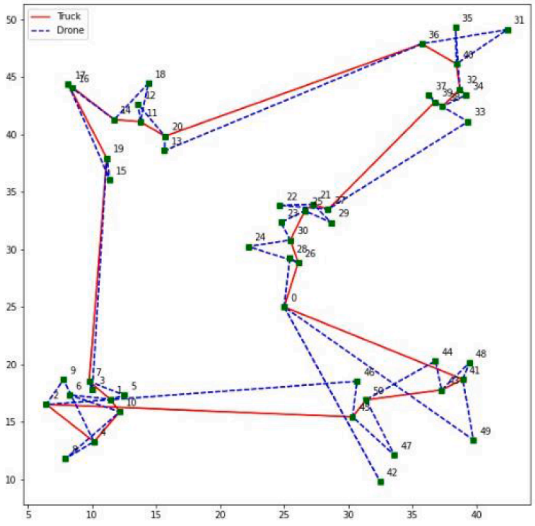

b) Instance C04

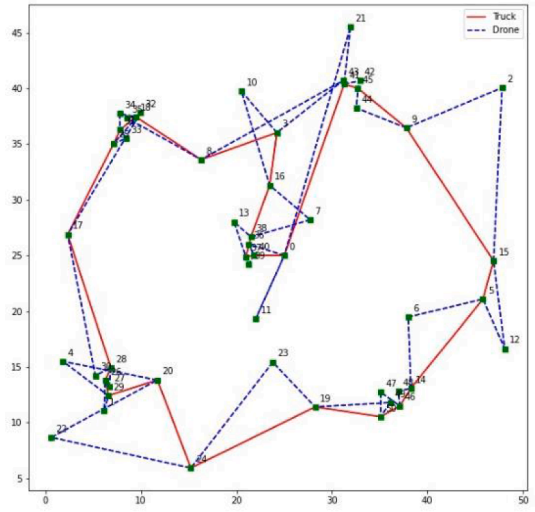

c) Instance RC04

Fig. 7. Solutions for instances with one sub-fleet and additional drone.

(*continued*)

Model parameters:	
x_{ijk}^D	binary variable, = 1 if drone k travels from node i to node j, 0 otherwise
y_{jk}	binary variable, = 1 if node j is a joint where drone k meets with the truck, 0 otherwise
z_{ik}^D	binary variable, = 1 if customer i is served by drone k, 0 otherwise
g_k^T	freight transported on truck k
g_{ik}^D	freight transported on drone k before visiting node i
g_{ik}^T	freight transported on truck k before visiting node i
a_{ik}^T	accumulated working time for truck k when arriving node i
a_{ik}^D	accumulated working time for drone k when arriving node i
w_{ik}^T	waiting time for truck k at joint i

The model formulation is the following.

$$min \sum_{i\in N}\sum_{j\in N:i\neq j}\sum_{k\in K}\left(c_{ij}^T x_{ijk}^T + c_{ij}^D x_{ijk}^D - c_{ij}^D x_{ijk}^T x_{ijk}^D\right) + \left(f^T + f^D\right)\sum_{j\in I}\sum_{k\in K} x_{Ojk}^T \tag{1}$$

s.t.

$$\sum_{j\in I:j\neq i} x_{ijk}^T \leq 1 \quad \forall k\in K, i\in N \tag{2}$$

$$\sum_{i\in N:i\neq l} x_{ilk}^T = \sum_{j\in N:j\neq l} x_{ljk}^T \quad \forall k\in K, l\in N \tag{3}$$

$$\sum_{j\in I:i\neq j} x_{ijk}^D \leq 1 \quad \forall k\in K, i\in N \tag{4}$$

$$\sum_{i\in N:i\neq l} x_{ilk}^D = \sum_{j\in N:l\neq j} x_{ljk}^D \quad \forall k\in K, l\in N \tag{5}$$

$$\sum_{j\in I} x_{Ojk}^T = \sum_{j\in I} x_{Ojk}^D \quad \forall k\in K \tag{6}$$

$$\sum_{i\in N:i\neq j} x_{ijk}^T = y_{jk} \quad \forall k\in K, j\in I \tag{7}$$

$$\sum_{i\in N:i\neq j} x_{ijk}^D \geq y_{jk} \quad \forall k\in K, j\in I \tag{8}$$

$$\sum_{i\in N:i\neq j}\left(x_{ijk}^D - y_{jk}\right) = z_{jk}^D \quad \forall k\in K, j\in I \tag{9}$$

$$\sum_{i\in N:i\neq j} x_{ijk}^T = 1 - z_{jk}^D \quad \forall k\in K, j\in I \tag{10}$$

$$\sum_{i\in N:i\neq j}\left(x_{ijk}^T + x_{ijk}^D\right) \leq 1 + y_{jk} \quad \forall k\in K, j\in I \tag{11}$$

$$\sum_{k\in K} y_{jk} \leq 1 \quad \forall j\in I \tag{12}$$

$$g_k^T \leq Q \quad \forall k\in K \tag{13}$$

$$g_k^T \geq \sum_{j\in I} g_{jk}^T + \sum_{j\in I} g_{jk}^D \quad \forall k\in K \tag{14}$$

$$g_{jk}^D = q_j\left(z_{jk}^D\right) \quad \forall k\in K, j\in I \tag{15}$$

$$g_{jk}^T = q_j\left(1 - z_{jk}^D\right) \quad \forall k\in K, j\in I \tag{16}$$

$$\sum_{k\in K}\left(\sum_{j\in I} g_{jk}^T + \sum_{j\in I} g_{jk}^D\right) = \sum_{j\in I} q_j \tag{17}$$

$$a_{ik}^T \leq T \quad \forall k\in K, i\in N \tag{18}$$

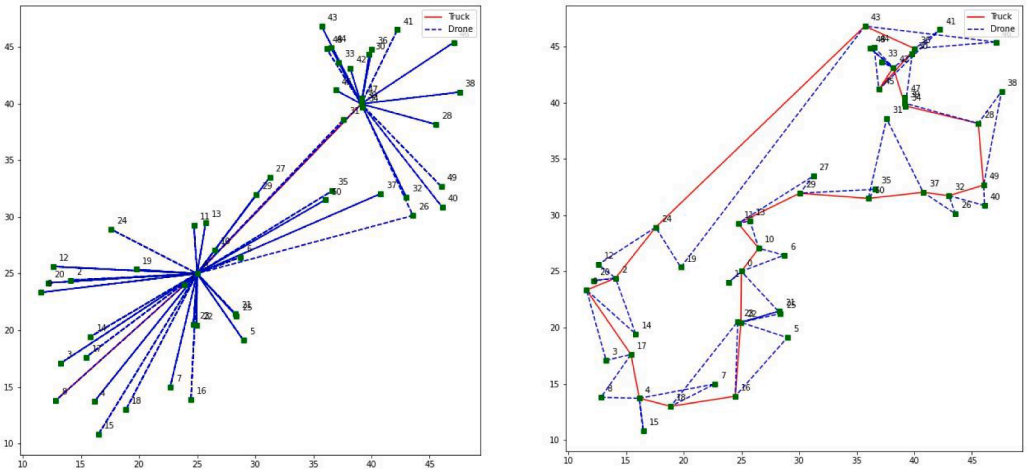

Fig. 8. Solution of instance C01 with different values for parameter π using FS^{+} mode.

Table 3
Output results of VRPD for FS, FS^{+}, and FS^{+1} methods.

Instances	FS		FS^{+}			FS^{+1}			△%Total Cost		
	SF	Total Cost	π	SF	Total Cost	π	SF	Total Cost	γ_1	γ_2	γ_3
C01	1	5271.32	0.3	1	5273.96	0.3	1	**5263.29**	0.05%	−0.15%	−0.20%
C02	2*	5865.63	0.2	2*	**5822.58**	0.1	2*	5894.99	−0.73%	0.50%	1.24%
C03	2	10271.19	0.8	2	**10171.39**	1	2	10254.77	−0.97%	−0.16%	0.82%
C04	2*	**5817.6**	1	2*	5824.24	0.7	2	10169.69	0.11%	74.81%	74.61%
C05	2	10223.31	0.3	2	10190.97	0.5	2	**10178.78**	−0.32%	−0.44%	−0.12%
C06	2	10286.3	0.2	2	10296.50	0.4	2	**10284.54**	0.10%	−0.02%	−0.12%
C07	2	10431.35	0.3	2	10409.12	0.3	2	**10406.04**	−0.21%	−0.24%	−0.03%
C08	2	**10431.97**	0.1	2	10433.25	0.1	2	10450.14	0.01%	0.17%	0.16%
C09	4	20604.9	0.1	4	20648.85	0.3	4	**20601.45**	0.21%	−0.02%	−0.23%
C10	4	20412.4	1	9**	**18668.31**	0.7	4	20364.22	−8.54%	−0.24%	9.08%
C11	4	20419.55	0.2	4	20424.10	0.5	4	**20340.55**	0.02%	−0.39%	−0.41%
C12	4	20539.88	0.1	4	20591.51	0.1	4	**20524.22**	0.25%	−0.08%	−0.33%
R01	2	10473.6	0.7	2	**10383.55**	0.7	2	10427.67	−0.86%	−0.44%	0.42%
R02	2	10377.84	0.8	2	**10351.50**	1	2	10372.25	−0.25%	−0.05%	0.20%
R03	2	10402.1	0.8	2	10363.59	1	2	**10356.25**	−0.37%	−0.44%	−0.07%
R04	2	10439.5	0.8	2	**10332.77**	1	2	10384.62	−1.02%	−0.53%	0.50%
R05	3	15659.83	0.5	3	**15597.47**	0.9	3	15618.67	−0.40%	−0.26%	0.14%
R06	3	15695.33	0.5	3	15624.17	0.7	3	**15618.71**	−0.45%	−0.49%	−0.03%
R07	3	15703.1	0.6	3	**15585.10**	0.6	3	15602.87	−0.75%	−0.64%	0.11%
R08	3	15640.82	0.5	3	15561.98	0.8	3	**15556.00**	−0.50%	−0.54%	−0.04%
R09	4	21086.26	0.1	4	**21004.52**	0.1	4	21108.37	−0.39%	0.10%	0.49%
R10	4	21101.61	0.2	4	**21005.23**	0.1	4	21099.53	−0.46%	−0.01%	0.45%
R11	4	**21006.22**	0.1	4	21069.37	0.1	4	21089.72	0.30%	0.40%	0.10%
R12	4	**21079.6**	0.1	4	21090.62	0.1	4	21100.88	0.05%	0.10%	0.05%
RC01	2	10310.85	0.3	2	10296.97	1	2	**10266.83**	−0.13%	−0.43%	−0.29%
RC02	2	10419.11	0.9	2	**10323.85**	1	2	10378.27	−0.91%	−0.39%	0.53%
RC03	2	10297.75	0.7	2	10250.24	0.8	2	**10223.54**	−0.46%	−0.72%	−0.26%
RC04	2*	**5836.5**	0.8	2	10200.24	0.1	2*	5852.17	74.77%	0.27%	−42.63%
RC05	3	**15420.14**	0.4	3	15454.60	0.9	3	15434.72	0.22%	0.09%	−0.13%
RC06	2	**10728.72**	0.1	3*	11145.33	0.1	2	10765.53	3.88%	0.34%	−3.41%
RC07	2	**10653.71**	0.6	3	15460.19	0.1	2	10723.67	45.12%	0.66%	−30.64%
RC08	3	15449.51	0.4	3	15418.75	1	3	**15392.56**	−0.20%	−0.37%	−0.17%
RC09	4	**20991.8**	0.2	4	21010.57	0.2	4	21085.41	0.09%	0.45%	0.36%
RC10	4	20890.32	0.2	4	20909.28	0.2	4	**20878.90**	0.09%	−0.05%	−0.15%
RC11	4	**20836.77**	0.1	4	20866.71	0.1	4	20840.60	0.14%	0.02%	−0.13%
RC12	4	20840.82	0.2	4	**20832.99**	0.3	4	20859.05	−0.04%	0.09%	0.13%

Note: *: Only one drone of the 2nd sub-fleet is dispatched; **: only one drone from the 4th to the 9th sub-fleet are dispatched; γ_1: (FS^{+} Total Cost - FS Total Cost)/(FS Total Cost); γ_2: (FS^{+1} Total Cost - FS Total Cost)/(FS Total Cost); γ_3: (FS^{+1}Total cost - FS^{+} Total Cost)/(FS^{+} Total Cost).

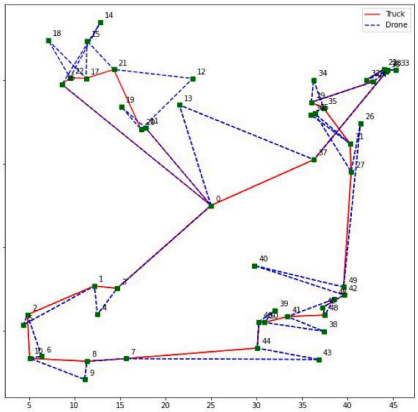

(a) FS Mode (Total Cost: 10,271.19)

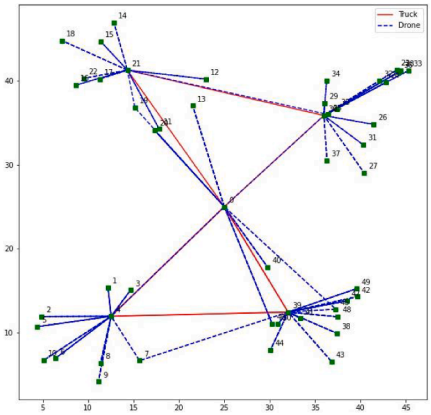

(b) FS^{+} Mode (Total Cost: 10,171.39)

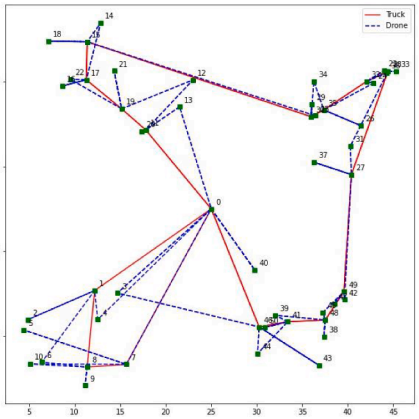

(c) FS^{+1} Mode (Total Cost: 10,254.77)

Fig. 9. Outputs of instance C03 for FS, FS^{+}, and FS^{+1} Modes.

$$w_{ik}^{T} \le W y_{ik} \quad \forall k \in K, i \in I \tag{19}$$

$$a_{jk}^{T} \ge \mathrm{r} + a_{ik}^{T} + s_{i}^{T} + w_{ik}^{T} + t_{ij}^{T} - T\left(1 - x_{ijk}^{T}\right) \quad \forall k \in K, i \in I, j \in N : i \ne j \tag{20}$$

$$a_{ik}^{T} \ge t_{Oj}^{T} - T\left(1 - x_{Ojk}^{T}\right) \quad \forall k \in K, j \in I \tag{21}$$

$$a_{ik}^{D} \le T \quad \forall k \in K, i \in N \tag{22}$$

$$a_{jk}^{D} \ge \mathrm{r} + a_{ik}^{D} + s_{i}^{D} + t_{ij}^{D} - T\left(1 - x_{ijk}^{D}\right) \quad \forall k \in K, i \in I, j \in N : i \ne j \tag{23}$$

$$a_{ik}^{D} \ge t_{Oj}^{D} - T\left(1 - x_{Ojk}^{D}\right) \quad \forall k \in K, j \in I \tag{24}$$

$$a_{Ok}^{D} \ge a_{Ok}^{T} \quad \forall k \in K \tag{25}$$

$$a_{ik}^{D} \ge a_{ik}^{T} - T(1 - y_{ik}) \quad \forall k \in K, i \in I \tag{26}$$

$$a_{ik}^{D} \le a_{ik}^{T} + s_{i}^{T} + W y_{ik} + T(1 - y_{ik}) \quad \forall k \in K, i \in I \tag{27}$$

$$F x_{ijk}^{T} \ge (t_{il}^{D} + s_{l}^{D} + t_{lj}^{D}) z_{lk}^{D} \quad \forall k \in K, i, l \in I : i \ne l, j \in N : j \ne l, j \ne i \tag{28}$$

$$a_{jk}^{D} \ge a_{ik}^{T} + s_{i}^{T} + w_{ik}^{T} + t_{il}^{D} + s_{l}^{D} + t_{lj}^{D} - T(1 - y_{ik}) \quad \forall k \in K, i, l \in I : i \ne l, j \in N : j \ne l, j \ne i \tag{29}$$

$$\sum_{i \in S} \sum_{j \in S} x_{ijk}^{T} \le |S| - 1 \quad \forall S \subseteq I, k \in K \tag{30}$$

$$\sum_{i \in S} \sum_{j \in S} x_{ijk}^{D} \le |S| - 1 \quad \forall S \subseteq I, k \in K \tag{31}$$

Table 4
Results of all instances for VRPD and VRP (only trucks).

Instance	NC	VRPD						VRP		Total Cost Differences		
		FS mode		FS^{+} mode		FS^{+1} mode						
		SF	Total Cost ($)	SF	Total Cost ($)	SF	Total Cost ($)	NT	Total Cost ($)	Δ_1	Δ_2	Δ_3
C01	50	1	5271.32	1	5273.96	1	5263.29	2	9266.531	43.1%	43.1%	43.2%
C02	50	2*	5865.63	2*	5822.58	2*	5894.99	2	9611.51	39.0%	39.4%	38.7%
C03	50	2	10271.19	2	10171.39	2	10254.77	2	9502.65	−8.1%	−7.0%	−7.9%
C04	50	2*	5817.60	2*	5824.24	2	10169.69	2	9437.06	38.4%	38.3%	−7.8%
C05	100	2	10223.31	2	10190.97	2	10178.78	3	13887.07	26.4%	26.6%	26.7%
C06	100	2	10286.30	2	10296.50	2	10284.54	4	18431.90	44.2%	44.1%	44.2%
C07	100	2	10431.35	2	10409.12	2	10406.04	4	18580.04	43.9%	44.0%	44.0%
C08	100	2	10431.97	2	10433.25	2	10450.14	4	18592.18	43.9%	43.9%	43.8%
C09	200	4	20604.90	4	20648.85	4	20601.45	7	32469.90	36.5%	36.4%	36.6%
C10	200	4	20412.40	9**	18668.31	4	20364.22	6	27645.41	26.2%	32.5%	26.3%
C11	200	4	20419.55	4	20424.10	4	20340.55	6	27790.61	26.5%	26.5%	26.8%
C12	200	4	20539.88	4	20591.51	4	20524.22	7	32240.10	36.3%	36.1%	36.3%
R01	50	2	10473.60	2	10383.55	2	10427.67	3	14175.99	26.1%	26.8%	26.4%
R02	50	2	10377.84	2	10351.50	2	10372.25	2	9635.14	−7.7%	−7.4%	−7.7%
R03	50	2	10402.10	2	10363.59	2	10356.25	2	9798.68	−6.2%	−5.8%	−5.7%
R04	50	2	10439.50	2	10332.77	2	10384.62	2	9735.61	−7.2%	−6.1%	−6.7%
R05	100	3	15659.83	3	15597.47	3	15618.67	4	19021.77	17.7%	18.0%	17.9%
R06	100	3	15695.33	3	15624.17	3	15618.71	4	18954.89	17.2%	17.6%	17.6%
R07	100	3	15703.10	3	15585.10	3	15602.87	4	19074.54	17.7%	18.3%	18.2%
R08	100	3	15640.82	3	15561.98	3	15556.00	4	19008.92	17.7%	18.1%	18.2%
R09	200	4	21086.26	4	21004.52	4	21108.37	7	32866.56	35.8%	36.1%	35.8%
R10	200	4	21101.61	4	21005.23	4	21099.53	7	32941.29	35.9%	36.2%	35.9%
R11	200	4	21006.22	4	21069.37	4	21089.72	7	32902.45	36.2%	36.0%	35.9%
R12	200	4	21079.60	4	21090.62	4	21100.88	7	32900.34	35.9%	35.9%	35.9%
RC01	50	2	10310.85	2	10296.97	2	10266.83	2	9605.45	−7.3%	−7.2%	−6.9%
RC02	50	2	10419.11	2	10323.85	2	10378.27	2	9711.33	−7.3%	−6.3%	−6.9%
RC03	50	2	10297.75	2	10250.24	2	10223.54	2	9613.95	−7.1%	−6.6%	−6.3%
RC04	50	2*	5836.50	2	10200.24	2*	5852.17	2	9523.62	38.7%	−7.1%	38.6%
RC05	100	3	15420.14	3	15454.60	3	15434.72	4	18790.52	17.9%	17.8%	17.9%
RC06	100	2	10728.72	3*	11145.33	2	10765.53	4	18826.16	43.0%	40.8%	42.8%
RC07	100	2	10653.71	3	15460.19	2	10723.67	4	18938.56	43.7%	18.4%	43.4%
RC08	100	3	15449.51	3	15418.75	3	15392.56	4	18791.35	17.8%	17.9%	18.1%
RC09	200	4	20991.80	4	21010.57	4	21085.41	7	32801.24	36.0%	35.9%	35.7%
RC10	200	4	20890.32	4	20909.28	4	20878.90	7	32592.93	35.9%	35.8%	35.9%
RC11	200	4	20836.77	4	20866.71	4	20840.60	7	32690.16	36.3%	36.2%	36.2%
RC12	200	4	20840.82	4	20832.99	4	20859.05	7	32617.13	36.1%	36.1%	36.0%

Note: NC: number of customers; SF: number of sub-fleets; NT: number of trucks; *: one drone of 2nd sub-fleet is dispatched; **: one drone from the 4th to the 9th sub-fleet is dispatched; Δ_1: (FS Total Cost - VRP Total Cost)/(FS Total Cost); Δ_2: (FS^{+} Total Cost - VRP Total Cost)/(FS^{+} Total Cost); Δ_3: (FS^{+1}Total cost - VRP Total Cost)/(FS^{+1} Total Cost).

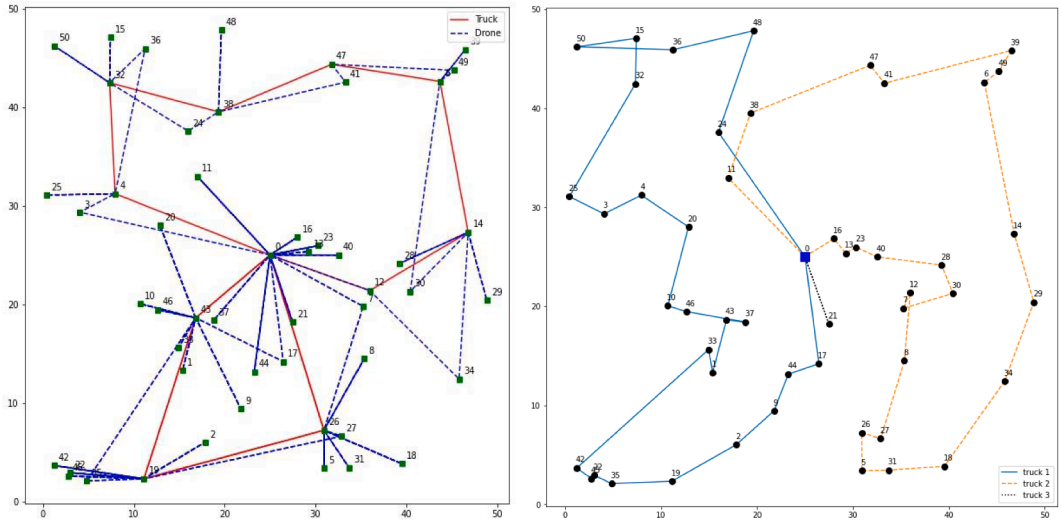

a) VRPD (Total Cost: $10,383.55) b) VRP (Total Cost: $14,175.99)

Fig. 10. Best solutions for instance R01 solving a) VRPD with FS^{+} mode and b) VRP (only trucks).

$$x_{ijk}^{T}, x_{ijk}^{D}, y_{jk}, z_{ik}^{D} \in \{0,1\} \quad \forall k \in K, i,j \in N : i \neq j \tag{32}$$

$$g_{k}^{T}, g_{ik}^{D}, a_{ik}^{T}, a_{ik}^{D}, w_{ik}^{T} \geq 0 \quad \forall k \in K, i \in N \tag{33}$$

The objective function (1) minimizes the total costs. The first term denotes the trucks' travel cost, the second term represents the drones' travel cost, the third term means that there is no travel cost of the drone when traveling on the truck, and the fourth and fifth terms consider the fixed costs of the trucks and drones, respectively. Constraints (2)-(6) ensure the flow balance of the trucks and drones. Constraints (2) and (3) determine routes for the trucks and Constraints (4) and (5) establish routes for the drones. Constraint (6) ensures that each dispatched truck from the depot has one corresponding drone. Constraint (7) indicates if a joint exists at node j, then the truck route must stop at this node. Constraint (8) indicates that if a joint exists at node j, then the corresponding drone must arrive at this node. Constraints (9)-(11) denote that node j must be visited by only one vehicle k or by both vehicles if this node is a joint. Constraint (12) ensures that node j may be enabled as only one joint.

Constraints (13)-(17) track the freight transported by trucks and drones. Constraint (13) ensures that the freight transported on a truck must not exceed its capacity. Constraint (14) ensures that the freight transported on a truck must be greater than or equal to the customer demands to be delivered in one vehicle route. Constraint (15) indicates that the freight on a drone must be equal to the customer demand at node j before visiting this node. Additionally, this constraint ensures that the freight on the drone must be zero before returning to the truck. Constraint (16) ensures that the customer demand of node j is served if this node is served by a truck. Constraint (17) ensures that all trucks and drones serve all the customer demands.

Constraints (18)-(29) ensure that the vehicles satisfy the time restrictions. Constraint (18) ensures that the accumulated working time of a truck is less than or equal to the total shift time. Constraint (19) ensures that the waiting time of a truck at joint is less than or equal to the maximum waiting time. Constraints (20) and (21) maintain the time continuity of each truck. Constraint (22) ensures that the accumulated working time of a drone is less than or equal to the total shift time. Constraints (23) and (24) maintain the time continuity of each drone. Constraint (25) ensures that a drone returns to the depot later than the truck if the drone has a mission or at the same time if the drone travels on the truck. Constraints (26) and (27) ensure that the arrival time of a drone at a joint must be within the time frame of the truck (time between arriving and leaving the joint). Constraint (28) indicates that a drone's flying time for one trip must be less than or equal to its maximum flying or working time. Constraint (29) ensures that the departure time of a drone from a joint corresponds to when the truck leaves the joint. Constraints (30) and (31) are the sub-tour elimination constraints for trucks and drones, respectively. Finally, constraints (32) and (33) indicate the domain of the decision variables.

In the FS mode shown in Fig. 1, the drone may visit only one customer while the accompanying truck travels from one customer to another customer. The use of drones is known to be much faster and cost-effective in delivering operations, as aforementioned. Therefore, the proposed FS method is revised to determine whether the total costs can be reduced if a drone visits more customers while the truck halts at a certain customer location. Hence, the drone has a third action in addition to the stationary and in-flight actions of the FS mode, as depicted in Fig. 3. This figure depicts that a truck waits at a customer's location in node A while the drone visits customers $\times$,y, and z.

A novel FS^{+} method was elaborated so that the drone serves multiple feasible customers as the truck waits at a customer location. A parameter π is designed to control the number of customers that a drone may serve during the truck's stop. The mechanism should consider that the flight times of the drone between the truck and the customers plus the customers' service time must be less than or equal to the drone's maximum flying or working time multiplied by parameter π. This constraint named "excess halt" is avoids an excessive truck idle time at one location.

An additional novel method called FS^{+1} is proposed to prevent the excess halt situation, where the drone may visit at most one customer during the truck's halt. Parameter π is also employed in this mode to control the maximum working time of the drone. Fig. 4 presents an example of the FS^{+1} method, where a drone serves a single customer u while the truck waits at node B.

For both FS^{+} and FS^{+1} modes, Constraint (4) of the model formulation presented above needs to be replaced by constraint (34) to allow the drone to serve multiple feasible customers while the truck waits at the same location, where M is a large positive number for the FS^{+} mode and $M = 2$ for the FS^{+1} mode.

$$\sum_{j \in I: i \neq j} x_{ijk}^{D} \leq M \quad \forall k \in K, i \in N \tag{34}$$

Constraint (19) is replaced by the constraint (35) to restrict the maximum waiting time of the truck at joint i.

$$w_{ik}^{T} \leq \pi W y_{ik} \quad \forall k \in K, i \in I \tag{35}$$

Constraint (27) is modified as constraint (36) to restrain the drone from arriving to joint i when the truck is not situated at such joint.

$$a_{ik}^{D} \leq a_{ik}^{T} + s_{i}^{T} + \pi W y_{ik} + T(1 - y_{ik}) \quad \forall k \in K, i \in I \tag{36}$$

Additionally, time constraint (37) is required for the FS^{+} and FS^{+1} modes to restrict the departure of the drone after serving customer l from joint i and returning to the same joint i.

$$a_{ik}^{D} \leq a_{ik}^{T} + s_{i}^{T} + \pi W + t_{il}^{D} + s_{l}^{D} + t_{li}^{D} - T(1 - y_{ik}) \quad \forall k \in K, i,l \in I : i \neq l \tag{37}$$

4. Methodology

ACO is an ant algorithm inspired by the food-foraged behavior of ants to solve path-finding problems. In this algorithm, ants exploit pheromone information deposited on edges of a graph to obtain shortest paths between food sources and their nests [52]. Dorigo and Gambardella [53] presented a metaheuristic algorithm called the Ant Colony System (ACS) that is constituted by three main procedures: selection scheme, local pheromone update, and global pheromone update. Our solving process of the VRPD is based on ACS, considering that each ant trip represents a vehicle route. First, the mechanism for selecting edges on a route is described by Eq. (38), in which an ant at node i chooses to visit the next customer j probabilistically favoring those nodes that connect short edges and larger amount of pheromone.

$$S = \begin{cases} \max\limits_{j \in \Omega} \{Att_{ij}\} & if \;\; q \leq q_0 \\ p_{ij} & otherwise \end{cases} \tag{38}$$

where Ω_i is the set of feasible customers to be served by an ant at node i, parameter q_0 is a predefined real number ($0 \leq q_0 \leq 1$) to determine whether the ant chooses to explore new edges or exploit a priori and

accumulated knowledge, q is a random number ranged between 0 and 1, p_{ij} is the state transition probability, and Att_{ij} indicates the attraction of an edge between nodes i and j for an ant located at node i using Eq. (39).

$$Att_{i,j} = (\tau_{ij})^{\alpha}(\eta_{ij})^{\beta} \tag{39}$$

where τ_{ij} and n_{ij} denote the pheromone intensity and visibility, respectively. The visibility is defined as the reciprocal of the distance between nodes i and j multiplied by M, where M is a constant used to adjust the visibility value. Additionally, α and β are used for weighting the pheromone intensity and visibility, respectively. The probabilistic choice of the next edge for an ant will be updated as the ant decides to explore a new edge according to Eq. (33). The probability of an ant selecting a feasible edge between nodes i and j is calculated using the state transition probability p_{ij} with Eq. (40).

$$p_{ij} = \begin{cases} \dfrac{Att_{ij}}{\sum_{k\in\Omega_i} Att_{ik}} & \forall j \in \Omega_i \\ 0 & \forall j \notin \Omega_i \end{cases} \tag{40}$$

Second, the pheromone level on the edges is modified once an ant completes its tour by applying the local pheromone update rule with Eq. (41).

$$\tau_{ij} = (1-\rho)\bullet\tau_{ij} + \rho\bullet\tau_0 \tag{41}$$

where τ_{ij} is the pheromone level on the edge between nodes i and j, ρ is a parameter that indicates the pheromone evaporation rate, and $\tau_0$is the initial pheromone trail intensity. During this local pheromone update, proportion ρ of the previously deposited pheromone is evaporated, and proportion $(1-\rho)$ of the pheromone level remains on the edges.

Third, the global pheromone update is triggered once all ants have completed their tours. In this update, the pheromone intensity is reset on all edges to encourage the ants to search for routes in the vicinity of the current best route. Subsequently, an extra amount of pheromone is allocated on the edges using Eq. (42), constituting the current best solution. In this equation, $J_{\psi^{gl}}$ is the cost of the current best route ψ^{gl}.

$$\tau_{ij} = (1-\rho)\tau_{ij} + \rho/J_{\psi^{gl}}(i,j) \in \psi^{gl} \tag{42}$$

Fig. 5 presents the flowchart of the ACO solving process for solving the VRPD. First, a graph is created that contains all nodes and edges, and the indices for the ants and iterations are initialized with zero values. Constants A and ITE indicate the total number of ants and total number of iterations, respectively, and ψ denotes the solution obtained by the current ant. When an ant is initialized, the vehicles are dispatched one by one until all the customers are served. In this case, a vehicle or sub-fleet denotes a composition of one truck and one drone (i.e., truck-drone pair). The drone actions are determined by the parameter z. Parameter ς is a randomly generated number, and its value ranges between 0 and 1. If $\varsigma < z$ holds, then the drone will travel on the truck until the next customer; otherwise, the drone has the mission to serve the following customer, and subsequently, return to the truck. The drone's departure time at a joint is the same as the truck's departure time. When an ant completes its tour by serving all customers, the solution found is compared and replaced by the existing optimal solution if this solution is better than the optimal solution. The local pheromone update mechanism is triggered to update the pheromone on the edges while additional ants are being dispatched. Once all ants have been dispatched, the global pheromone update mechanism is executed and a new iteration is initiated. The solving process is stopped as soon as the total number of iterations is equal to the predefined number ITE. If N is the total number of customers, then the time complexity of the ACO is $O(N^2)$ since it is executed N times to serve all customers.

This research employs the 2-opt method for the local search as soon as the solving process finds a solution. Fig. 6 illustrates the application of the 2-opt method to a truck-drone route. Conventionally, the new route gained by this method is to reverse the order of the customers between customers a and d in the truck route. However, customers x and z in the drone route must be reversed as well to maintain the solution feasibility for both truck and drone routes.

Subsequently, the drone route must be examined to verify if any of the drones violate the arrival time rule (See Fig. 2). If the rule is violated, then the solution must be abandoned. Otherwise, the cost will be recalculated to determine if a better solution has been found. This method is applied to any truck-drone route iteratively until a better solution is yielded or remains the same if all combinations are verified.

5. Computational tasks

Since the VRPD is a FVRP type, we adopted the benchmark created by Huang et al. [2] to verify the performance of the proposed ACO solving process. The dataset consists of three subsets, in which the customers are located in clusters (C), randomly (R), a combination of random and clusters (RC). Each subset contains 12 instances with 50, 100, and 200 customers. The instances of each subset are indexed from 01 to 12. Customerś demands and locations are given. The maximum truckload is set to 500 units of capacity, and the maximum working time of the truck is set to 480 units of time. The speed ratio of the drone and the truck is 50/35 (1.43). The fixed cost of one truck and one drone is set to 4360 and 436 units of money, respectively. Additionally, the travel cost per unit of distance of a truck and a drone are 3.3 and 0.33, respectively. If a drone serves a customer, then the service time is assumed to be equal to half of the truck's service time. Moreover, the maximum working time of a drone is set to 30 units of time. The truck's waiting endurance is set to 15 units of time, and the recovery time of the drone is 1 unit of time. The parameter settings of ACO are as follows: parameter q_0 is equal to 0.3, evaporation rate ρ is equal to 0.1, and the number of ants and iterations are equal to 30 (A = 30, ITE = 30). In addition, the parameter z has a maximum value of 0.3.

5.1. Comparison between ACO and optimal solutions for small instances

To assess the performance of the proposed ACO solving process, 18 small-size problems (grouped in R, C, RC) were designed and solved to optimality by using IBM CPLEX 12.10 solver. Table 1 presents the output results for comparing the proposed ACO solving process with the optimization model for the VRPD (FS mode) for small instances between 5 and 30 customers. This table shows that only one sub-fleet (i.e., one truck-drone pair) is required for both ACO and exact solutions for all instances, and that ACO yields equal or very similar total costs (within 1%) to the mathematical model results for most instances. Furthermore, the CPU time required to obtain the ACO results is considerably smaller than the exact results. Optimal solutions are obtained for 5 and 10 customers for all group distributions, and low integrality gap values of the feasible solutions are obtained after 7200 s of execution for 15 or more customers. Since optimal solutions are difficult to obtain for larger instances (VRPD is NP-hard), these results suggest that the proposed ACO provides competitive solutions within reasonable computing times.

5.2. ACO results with large instances

Table 2 presents the best output results for all instances with the three group distributions using the proposed ACO solving process. After solving with different α and β combinations, the best result of each combination is reported in this table for each instance. The results for instances C02, C04, and RC04 require two sub-fleets, but the second sub-fleet (denoted with an asterisk) is comprised by only one drone that has a mission to serve a single customer. Fig. 7a), 7b), and 7c) show the solution for instances C02, C04, and RC04, respectively. In these solutions, after the first sub-fleet returns to the depot, only one customer still needs to be serviced (customer #33 for instance C02, customer #42 for instance C04, and customer #11 for instance RC04). Thus, a second sub-fleet consisting of only one drone (truck is not required) is launched from the depot to serve this customer and then is returned to the depot.

The following managerial insights are withdrawn from the results in Table 2: i) the traveled distances, the number of sub-fleets, and the execution time tend to increase with the number of customers in each instance; ii) the total costs for instances with R group are higher than instances belonging to the C group (on average 34.7% higher for 50 customers and 34.0% higher for 100 customers) and RC group (on average 11.6% higher for 50 customers and 16.7% higher for 100 customers), particularly due to larger distances between randomly located customers; iii) on average, there are relatively low differences (less than 3%) between the total costs of the three group distributions for large instances with 200 customers; and iv) drones must travel longer distances than the trucks to serve their assigned customers since in this study the total costs of the drone are equal to 10% of the total costs of the truck, and the drones are 1.43 times faster than the trucks.

5.3. Comparison results using FS, FS^{+}, and FS^{+1} modes

Fig. 8a) presents the output result of instance C01 for $\pi = 1$ using FS^{+} mode, representing a maximum working time of the drone of 30 units of time with a total cost is 10,541.86. This result is much larger than the solution obtained with the FS method (5,271.32 in Table 2). In this case, the truck's efficacy is not fully employed since the truck idles for long periods of time at customer locations. There may be an excess halt while trying to take advantage of the drone's higher speed and lower travel cost. Thus, the usage of the truck and the drone must be balanced to approach the best cost-effectiveness in the results. The excess halt situation is controlled by adjusting the dronés maximum working time at a node through parameter π. The number of customers served by a drone during a truck's halt can be reduced by decreasing this parameter. For example, if π is reduced to 0.3 for instance C01, then the trucks halt is decreased, resulting in a total cost of 5,273.96 for FS^{+} mode, as shown in Fig. 8b). Both truck and drone are assigned customers in a more balanced manner. The total costs for the benchmark with parameter π varying between 0.1 and 1 using FS^{+} and FS^{+1} modes are presented in Tables A1 and A2, respectively, in the appendix.

Table 3 lists the results of the benchmark solved by FS, FS^{+}, and FS^{+1} methods. Different values of π were tested, and the best results for each instance are reported in bold. These results suggest that, for the studied instances, FS^{+1} is better suited for subset C, FS^{+} for subset R, and FS for subset RC since 58.3% of the instances in the C group presented the lowest cost with the FS^{+1} method, 58.3% of the instances in the R group with the FS^{+} method, and 50% of instances in the RC group with the FS^{+1} method. On average, larger distances among customers in the R group favor the use of drones due to their higher speed and more economical cost than the trucks, as in the FS^{+} mode. In the RC group, different distances are perceived between the customers. Hence, the dispatching truck-drone units used in the FS mode are sufficiently flexible to serve customers considering that the drones must arrive after the trucks at the customer locations. Lastly, when the customers are clustered in space, the drones accommodate their visits to a single customer while the trucks wait at a customer location.

Overall, Table 3 shows that the differences between the results (i.e., γ_1, γ_2, and γ_3) are less than 1%, except for those instances that require the use of an additional truck or sub-fleet (instances C04, RC04, and RC07). For example, for instance C04, the total cost increases in 74.81% when using FS^{+1} mode with respect to the FS mode. This significant increase in the total costs is due particularly to the fixed costs associated to the use of an additional truck for servicing the customers. In the FS^{+1} mode, the drone can serve at most one customer while the truck is halted. Therefore, in this instance, a second truck must be dispatched to serve the additional customers.

Additionally, in Table 3, the FS^{+} result of instance C10 shows that three truck-drone units and six single drones are required for servicing the customers. In this particular case of clustered customers, many customers are rapidly served by six drones directly from the depot instead of collaborating with a truck.

To further compare the methods, Fig. 9a), 9b), and 9c) illustrate the output results of instance C03 with FS, FS^{+}, and FS^{+1} modes, respectively. The truck and drone travel distances are equal to 180.63 and 251.8, respectively, for FS mode; 109.11 and 664.67, respectively, for FS^{+} mode; and 163.87 and 369.63, respectively, for FS^{+1} mode. When comparing between the modes, the FS mode uses mostly the truck, and the FS^{+} mode takes more advantage of the drone. Additionally, the FS^{+1} mode seems more balanced in the usage of the truck and the drone than the other two modes. For this specific instance, the FS^{+} mode yields the best solution with the lowest total cost of 10,171.39.

5.4. Comparison of VRPD with VRP

A comparison was performed between the VRPD and the VRP (truck only) using the benchmark, as shown in Table 4. For large instances with over 100 customers, this table shows that the cost-savings are on average more than 30%, suggesting that the VRPD produces a significant improved cost-savings compared to the typical VRP with truck-only delivery, similarly to Sacramento et al. [29]. For example, Fig. 10a) and 10b) show the best solutions for instance R01 using FS^{+} mode and VRP, respectively, where on average a cost-savings of 26.4% exists when servicing customers with two truck-drone units instead of three trucks. However, when the instances are smaller (50 customers), there is a tendency for the VRP to be more economical than VRPD. A possible cause of this trend is that the dronés parameter values that are used to solve the VRPD with the benchmark may differ from those employed in the real world. For example, the ratio between the total costs of the drone and truck are set to 1/10, which may vary depending on the type and brand of drone. Further research is required to have a deeper understanding of the cost differences between VRP and VRPD for small instances.

6. Conclusions

This research contributes to the existing literature by proposing an ACO algorithm to solve the VRPD with the FS mode. The ACO solving process for the VRPD yields the number of sub-fleets (i.e., dispatching truck-drone units) and optimal routes while minimizing total costs. Test experiments were implemented to examine the ACO performance in the resolution of the VRPD for instances with different sizes and group distributions (R, C, and RC). The results provide managerial insights related to the the total cost variation depending on the number and locations of customers. Overall, the drone is less expensive and faster than the truck. If the drone is fully utilized, then the drone is able to reduce the total logistic costs and improve the performance of delivery operations. When the drone accompanies the truck, the coordination of drone and truck has to be well-designed so that the delivery operations can be facilitated. This study provides promising truck-drone coordination operations to take full advantage of the drones.

Two novel modes are elaborated to solve the VRPD, which consists of servicing multiple feasible customers (FS^{+} mode) and only one feasible

customer (FS^{+1} mode) by drones while the trucks wait at customer locations. The results indicate that each mode has its merit and highlights another contribution of this study. The FS^{+1} mode performs better with instances from the C group, the FS^{+} mode with instances from the R group, and the FS mode with instances from the RC group.

The VRPD results with the three modes are compared with the VRP using the benchmark. Overall, the VRPD presents cost-savings over 30% for large size instances when compared to the VRP. In addition, the ACO results were compared to the optimal results for small instances, yielding promising results in a reasonable time period.

Some situations should be considered for future research. First, a drone may not fulfill a customer's need in one delivery, which means that a customeŕs demand may be greater than the drone's capacity. Additionally, some customers may be served only by a truck when the drone does not have a landing place or the customer is located in a no-flight zone. Different drone brands have different unit travel costs depending on their flying ranges, speeds, and capacities. These discriminations between drones could conduce to different conclusions. Further research should also investigate situations when a truck is accompanied by more than one drone, and when a drone is allowed to return to a different truck after servicing customers.

Declaration of Competing Interest

The authors declare that they have no known competing financial interests or personal relationships that could have appeared to influence the work reported in this paper.

Acknowledgement

The authors would like to thank the editor and the anonymous reviewers for their valuable comments and suggestions to improve the quality of the paper. Dr. Shan-Huen Huang would like to thank the Ministry of Science and Technology, Taiwan for the financial support (Project No. 109-2221-E-992-005).

Funding

This work was supported by the Ministry of Science and Technology, Taiwan [Project No. 109-2221-E-992-005].

Appendix A

Tables A1 and A2.

Table A1
Total costs per instance for different π values using the FS^{+} mode.

Instance	Parameter π									
	0.1	0.2	0.3	0.4	0.5	0.6	0.7	0.8	0.9	1
C01	5285.60	5284.70	**5273.96**	10100.71	10038.84	10060.03	10052.39	10018.52	5696.90	10541.86
C02	5914.00	**5822.58**	10225.15	10235.13	10257.28	10278.11	10250.27	10221.80	10208.48	10713.18
C03	10299.24	10284.46	10254.18	10244.67	10251.04	10217.84	10182.16	**10171.39**	10204.25	10705.42
C04	10207.01	10216.05	10184.87	10166.58	10182.67	10127.25	10137.42	10153.17	10176.00	**5824.24**
C05	10221.95	10192.48	**10190.97**	15148.74	15123.63	15147.93	19984.29	15690.98	15655.09	16213.75
C06	10311.48	**10296.50**	10301.30	15208.65	15148.14	15130.63	19972.89	15650.44	15610.49	15654.41
C07	10456.58	10423.54	**10409.12**	15349.50	15263.95	15265.18	20160.54	20140.38	15747.72	16293.40
C08	**10433.25**	10460.35	15313.41	15186.08	15308.32	15320.26	15788.02	20113.10	15682.45	15714.00
C09	**20648.85**	20667.87	21034.87	25429.71	30330.51	35234.08	30851.44	31339.06	27161.93	27660.45
C10	20435.80	20413.25	20373.85	25240.48	30097.20	25689.89	30734.03	26807.92	22528.54	**18668.31**
C11	20504.54	**20424.10**	20442.90	25425.99	30331.78	30355.23	35241.95	30798.55	26622.29	27484.13
C12	**20591.50**	20591.82	25397.92	25219.69	30260.74	25952.31	30724.47	30789.60	26376.35	26967.95
R01	10499.46	10499.42	10498.07	10479.06	10453.70	10430.48	**10383.55**	10425.54	15220.54	10884.99
R02	10399.23	10403.61	10402.44	10382.49	10407.75	10389.66	10378.15	**10351.50**	15255.69	10788.63
R03	10426.47	10403.20	10418.35	10390.32	10418.70	10382.10	10384.02	**10363.59**	10809.67	15228.61
R04	10431.17	10452.57	10473.00	10438.72	10416.35	10365.02	10388.56	**10332.77**	10480.25	10749.55
R05	15705.21	15727.59	15699.53	15626.79	**15597.47**	15715.47	20422.46	20461.48	20898.31	16471.71
R06	15718.97	15720.92	15679.18	15655.25	**15624.17**	20527.27	20473.22	20443.22	16084.67	20923.67
R07	15728.19	15714.97	15706.66	15641.30	15588.83	**15585.10**	20394.98	20400.48	16137.22	16462.32
R08	15712.09	15695.41	15641.93	15633.81	**15561.98**	15654.66	20472.82	20471.20	16065.60	20920.24
R09	**21004.52**	21105.40	25884.93	25795.72	30673.60	35535.01	31180.70	36068.72	31784.86	32260.34
R10	21101.81	**21005.22**	25928.31	25898.44	30706.13	35626.18	31325.47	36095.37	31784.15	32272.48
R11	**21069.37**	21083.13	25864.31	25852.43	30709.66	35596.45	35613.55	36130.99	31832.93	32280.49
R12	**21090.62**	21135.80	25891.16	25866.72	30721.01	35597.05	31222.93	36079.08	32191.60	27839.18
RC01	10310.36	10325.87	**10296.97**	10305.54	10305.88	10327.01	10320.43	10340.69	10388.97	10737.77
RC02	10432.58	10433.55	10469.09	10424.30	10377.30	10351.66	10336.16	10349.58	**10323.85**	10797.80
RC03	10347.52	10285.49	10293.11	10319.89	10301.99	10289.33	**10250.24**	10261.69	10256.20	10739.20
RC04	10248.32	10222.27	10263.81	10207.43	10250.82	10203.36	10230.81	**10200.24**	10220.92	10708.21
RC05	15478.60	15467.77	15456.92	**15454.60**	15459.72	15612.13	20330.10	20283.64	15845.54	16396.02
RC06	**11145.33**	11155.50	15529.49	15522.81	15490.94	15459.31	20336.56	15919.91	15907.21	15916.00
RC07	15586.89	15486.21	15531.49	15543.71	15502.80	**15460.19**	20309.85	20288.85	15833.11	15944.58
RC08	15474.28	15485.85	15441.90	**15418.75**	15501.08	15445.07	15482.22	20250.31	15792.19	16337.90
RC09	21030.81	**21010.57**	25797.43	25738.75	30563.04	35495.31	31095.99	36021.88	31655.46	27778.11
RC10	20918.74	**20909.28**	25710.73	25653.64	30492.77	26182.07	30928.11	30964.88	26586.26	26998.23
RC11	**20866.71**	20883.10	25722.98	25680.07	30562.91	30525.37	35418.26	30916.72	31443.98	22791.03
RC12	20860.38	**20832.99**	25716.00	25647.80	30561.39	30510.39	26130.85	30891.21	26455.39	26910.50

Note: Numbers in bold indicate lowest total cost per instance.

Table A2
Total costs per instance for different π values using the FS^{+1} mode.

Instance	Parameter π									
	0.1	0.2	0.3	0.4	0.5	0.6	0.7	0.8	0.9	1
C01	5266.275	5282.157	**5263.287**	10074.08	10092.91	10095.68	10087.71	10102.17	10100.71	10104.21
C02	**5894.986**	5945.977	10232.95	10237.5	10254.28	10233.78	10221.46	10241.93	10268.36	10264.23
C03	10294.54	10287.16	10260.86	10277.8	10266.82	10256.38	10256.34	10259.65	10260.49	**10254.77**
C04	10216.25	10216.18	10197.34	10195.92	10181.36	10174.41	**10169.69**	10175.76	10186.78	10184.51
C05	10235.56	10196.59	10207.64	10226.03	**10178.78**	10245.46	10241.70	10242.25	10238.63	10204.31
C06	10306.52	10308.78	10292.00	**10284.54**	10751.80	10708.78	10697.91	10352.20	10711.94	10710.34
C07	10455.82	10423.16	**10406.04**	10423.57	10407.40	10853.98	10826.00	15269.54	10889.35	10839.72
C08	**10450.14**	10455.44	10960.29	15310.63	15293.19	15307.43	15262.45	15267.01	15270.58	15268.88
C09	20670.58	20619.1	**20601.45**	20707.05	25494.26	25512.24	25500.65	25508.57	25471.37	25454.14
C10	20417.68	20416.77	20366.86	20371.83	20388.50	20365.97	**20364.22**	20391.76	20386.87	20398.23
C11	20515.40	20459.88	20370.26	20354.64	20340.55	20366.87	20371.28	20360.91	**20349.83**	20376.30
C12	**20524.22**	20595.54	20557.27	20590.42	20527.06	20645.68	25409.19	25344.85	20920.34	25366.91
R01	10490.40	10511.77	10490.00	10482.50	10453.99	10449.40	**10427.67**	10436.20	10428.35	10442.79
R02	10409.33	10412.21	10407.66	10390.08	10404.40	10404.67	10410.24	10403.66	10414.66	**10372.25**
R03	10412.08	10429.22	10421.67	10410.17	10419.45	10396.55	10373.98	10368.54	10356.79	**10356.25**
R04	10479.41	10457.78	10450.78	10438.24	10403.18	10396.49	10412.27	10395.38	10390.88	**10384.62**
R05	15696.21	15712.48	15709.48	15650.72	15652.20	15659.72	15667.30	15667.38	**15618.67**	15633.31
R06	15729.35	15724.98	15719.84	15660.73	15670.14	15642.90	**15618.71**	15656.26	15630.97	15661.55
R07	15751.21	15731.77	15614.89	15632.59	15674.67	**15602.87**	15611.33	15660.00	15637.63	15634.00
R08	15677.90	15677.75	15655.31	15615.27	15625.23	15618.53	15609.22	**15556.00**	15593.28	15609.65
R09	**21108.37**	21152.16	25868.47	25792.33	25881.80	25839.43	25851.92	25849.11	25846.45	25846.31
R10	**21099.53**	21107.17	25918.52	25906.76	25866.71	25899.06	25916.14	25905.55	25897.77	25914.28
R11	**21089.72**	21226.06	25861.73	25858.71	25835.62	25863.08	25792.43	25833.37	25849.51	25851.53
R12	**21100.88**	21636.93	25911.40	25908.41	25872.21	25880.89	25799.53	25869.79	25880.53	25886.56
RC01	10329.78	10293.95	10297.43	10267.07	10322.48	10330.48	10297.63	10333.58	10273.67	**10266.82**
RC02	10435.92	10434.67	10441.07	10424.83	10421.49	10410.27	10395.05	10392.65	10392.21	**10378.27**
RC03	10344.29	10330.42	10282.42	10297.78	10312.67	10303.68	10316.42	10223.54	10290.19	10301.75
RC04	**5852.17**	10224.45	10227.99	10229.78	10228.07	10208.55	10195.74	10209.20	10209.86	10210.14
RC05	15470.94	15488.23	15484.10	15458.44	15451.23	15442.50	15437.91	15443.82	**15434.72**	15440.14
RC06	**10765.53**	11126.42	15510.97	15487.56	15490.65	15500.68	15489.08	15514.35	15502.22	15475.65
RC07	**10723.67**	15545.55	15536.76	15532.12	15546.93	15528.60	15517.57	15522.14	15512.15	15479.28
RC08	15472.59	15479.33	15499.44	15478.90	15469.76	15430.68	15411.57	15404.81	15400.65	**15392.56**
RC09	21088.72	**21085.40**	25794.20	25765.45	25731.28	25766.83	25751.83	25763.56	25743.93	25767.50
RC10	20904.97	**20878.90**	21377.77	25707.58	25716.98	25698.10	25637.32	25695.76	25690.91	25683.00
RC11	**20840.60**	20849.52	20921.16	21227.02	25696.25	25640.00	25641.05	25632.92	25629.66	25659.03
RC12	20879.49	20891.41	**20859.05**	20895.56	25665.78	25650.64	25667.50	25687.71	25621.56	25688.31

References

[1] IMARC Group, Logistics Market: Global Industry Trends, Share, Size, Growth, Opportunity and Forecast 2021–2026, 2020. https://www.imarcgroup.com/logistics-market.

[2] Y.H. Huang, C.A. Blazquez, S.H. Huang, G. Paredes-Belmar, G. Latorre-Nunez, Solving the feeder vehicle routing problem using ant colony optimization, Comput. Ind. Eng. 127 (2019) 520–535.

[3] J. Li, E. Rombaut, L. Vanhaverbeke, A systematic review of agent-based models for autonomous vehicles in urban mobility and logistics: Possibilities for integrated simulation models, Comput. Environ. Urban Syst. 89 (2021), 101686.

[4] B. Rabta, C. Wankmüller, G. Reiner, A drone fleet model for last-mile distribution in disaster relief operations, Int. J. Disaster Risk Reduct. 28 (2018) 107–112.

[5] J. Scott, C. Scott, Drone Delivery Models for Healthcare, in: Proceedings of the 50th Hawaii International Conference on System Sciences, Waikoloa Village, Hawaii, USA, January 4–7, 2017. http://128.171.57.22/bitstream/10125/41557/1/paper0408.pdf.

[6] C. Murray, A. Chu, The flying sidekick traveling salesman problem: Optimization of drone-assisted parcel delivery, Transp. Res. Part C 54 (2015) 86–109.

[7] F. Giones, A. Brem, From toys to tools: The co-evolution of technological and entrepreneurial developments in the drone industry, Bus. Horiz. 60 (6) (2017) 875–884.

[8] E. Yurek, H. Ozmutlu, A decomposition-based iterative optimization algorithm for traveling salesman problem with drone, Transp. Res. Part C 91 (2018) 249–262.

[9] M. Casazza, A. Ceselli, A branch and price approach for the Split Pickup and Split Delivery VRP, Electr. Notes Discr. Math. 69 (2018) 189–196.

[10] Z. Wang, P. Wen, Optimization of a Low-Carbon Two-Echelon Heterogeneous-Fleet Vehicle Routing for Cold Chain Logistics under Mixed Time Window, Sustainability 12 (2020) 1967, https://doi.org/10.3390/su12051967.

[11] A. Azadeh, H. Farrokhi-Asl, The close–open mixed multi depot vehicle routing problem considering internal and external fleet of vehicles, Transp. Lett. 11 (2) (2019) 78–92.

[12] M.E.H. Sadati, D. Aksen, N. Aras, The r-interdiction selective multi-depot vehicle routing problem, Int. Trans. Operat. Res. 27 (2020) 835–866.

[13] H.K. Chen, Issues for the linehaul-feeder vehicle routing problem with virtual depots and time windows, J. Eastern Asia Soc. Transp. Stud. 11 (2015) 678–692.

[14] C. Brandstaetter, M. Reimann, The Line-haul Feeder Vehicle Routing Problem: Mathematical model formulation and heuristic approaches, Eur. J. Oper. Res. 270 (2018) 157–170.

[15] S. Poikonen, B. Golden, Multi-visit drone routing problem, Comput. Oper. Res. 113 (2020) 104802, https://doi.org/10.1016/j.cor.2019.104802.

[16] X. Wang, S. Poikonen, B. Golden, The vehicle routing problem with drones: several worst-case results, Optimiz. Lett. 11 (4) (2017) 679–697.

[17] G. Crişan, E. Nechita, On a cooperative truck-and-drone delivery system, Proc. Comput. Sci. 159 (2019) 38–47.

[18] F. Guerriero, R. Surace, V. Loscri, E. Natalizio, A multi-objective approach for unmanned aerial vehicle routing problem with soft time windows constraints, Appl. Math. Model. 38 (3) (2014) 839–852.

[19] S. Poikonen, X. Wang, B. Golden, The vehicle routing problem with drones: Extended models and connections, Networks 70 (1) (2017) 34–43.

[20] P. Kitjacharoenchai, S. Lee, Vehicle Routing Problem with Drones for Last Mile Delivery, Procedia Manuf. 39 (2019) 314–324.

[21] Z. Wang, J.-B. Sheu, Vehicle routing problem with drones, Transp. Res. Part B: Methodol. 122 (2019) 350–364.

[22] S. Chung, B. Sah, J. Lee, Optimization for drone and drone-truck combined operations: A review of the state of the art and future directions, Comput. Oper. Res. 123 (2020), 105004.

[23] J. Euchi, A. Sadok, Hybrid genetic-sweep algorithm to solve the vehicle routing problem with drones, Phys. Commun. 44 (2021) 101236. ISSN 1874-4907.

[24] D.R. Viloria, E. Solano-Charris, A. Muñoz-Villamizar, J. Montoya-Torres, Unmanned aerial vehicles/drones in vehicle routing problems: a literature review, Int. Trans. Operat. Res. Spec Iss. Transp. Log. Autonom. Technol. 28 (4) (2021) 1626–1657.

[25] K. Dorling, J. Heinrichs, G. Messier, S. Magierowski, Vehicle Routing Problems for Drone Delivery, IEEE Trans. Syst. Man Cybern. Syst. 47 (1) (2017) 70–85.

[26] X. Chu, S.X. Xu, F. Cai, J. Chen, Q. Qin, An efficient auction mechanism for regional logistics synchronization, J. Intell. Manuf. 30 (7) (2019) 2715–2731.

[27] A. Karak, K. Abdelghany, The hybrid vehicle-drone routing problem for pick-up and delivery services, Transp. Res. Part C 102 (2019) 427–449.

[28] Y. Liu, An optimization-driven dynamic vehicle routing algorithm for on-demand meal delivery using drones, Comput. Oper. Res. 111 (2019) 1–20.

[29] D. Sacramento, D. Pisinger, S. Ropke, An adaptive large neighborhood search metaheuristic for the vehicle routing problem with drones, Transp. Res. Part C 102 (2019) 289–315.

[30] D. Schermer, M. Moeini, O. Wendt, A matheuristic for the vehicle routing problem with drones and its variants, Transp. Res. Part C 106 (2019) 166–204.
[31] X. Chu, F. Cai, D. Gao, L. Li, J. Cui, S.X. Xu, Q. Qin, An artificial bee colony algorithm with adaptive heterogeneous competition for global optimization problems, Appl. Soft Comput. 93 (2020), 106391.
[32] Y.-Q. Han, J.-Q. Li, Z. Liu, C. Liu, J. Tian, Metaheuristic algorithm for solving the multi-objective vehicle routing problem with time window and drones, Intell. Manuf. Robot.-Res. Artic. (2020) 1–14.
[33] P. Kitjacharoenchai, B.-C. Min, S. Lee, Two echelon vehicle routing problem with drones in last mile delivery, Int. J. Prod. Econ. 225 (2020), 107598.
[34] L. Pugliese, G. Macrina, F. Guerriero, Trucks and drones cooperation in the last-mile delivery process, Networks 1–29 (2020), https://doi.org/10.1002/net.22015.
[35] S. Shao, S.X. Xu, G.Q. Huang, Variable neighborhood search and tabu search for auction-based waste collection synchronization, Transp. Res. Part B: Methodol. 133 (2020) 1–20.
[36] L. Nuryanti, A vehicle routing problem optimization with drone using tabu search algorithm and analytical hierarchy process, J. Ind. Technol. Assess. 15 (1) (2021) 64–69.
[37] J.E. Bell, P.R. McMullen, Ant colony optimization techniques for the vehicle routing problem, Adv. Eng. Inf. 18 (1) (2004) 41–48.
[38] S.H. Huang, P.C. Lin, A modified ant colony optimization algorithm for multi-item inventory routing problems with demand uncertainty, Transp. Res. Part E 46 (2010) 598–611.
[39] S.H. Huang, Y.H. Huang, C.A. Blazquez, G. Paredes-Belmar, Application of the ant colony optimization in the resolution of the bridge inspection routing problem, Appl. Soft Comput. 65 (2018) 443–461.
[40] X. Xiang, J. Qiu, J. Xiao, X. Zhang, Demand coverage diversity based ant colony optimization for dynamic vehicle routing problems, Eng. Appl. Artif. Intell. 91 (2020) 103582, https://doi.org/10.1016/j.engappai.2020.103582.
[41] E. Yakici, Solving location and routing problem for UAVs, Comput. Ind. Eng. 102 (2016) 294–301.
[42] F. Yan, Autonomous vehicle routing problem solution based on artificial potential field with parallel ant colony optimization (ACO) algorithm, Pattern Recogn. Lett. 116 (2018) 195–199.
[43] O. Yilmaz, E. Yakici, M. Karatas, A UAV location and routing problem with spatio-temporal synchronization constraints solved by ant colony optimization, J. Heurist. 25 (2019) 673–701.
[44] V. Horbulin, L. Hulianytskyi, I. Sergienko, Optimization of UAV Team Routes in the Presence of Alternative and Dynamic Depots, Cybern. Syst. Anal. 56 (2020) 195–203.
[45] S. Gao, J. Wu, J. Ai, Multi-UAV reconnaissance task allocation for heterogeneous targets using grouping ant colony optimization algorithm, Soft. Comput. 25 (2021) 7155–7167.
[46] J. Chen, F. Ye, Y. Li, Travelling salesman problem for UAV path planning with two parallel optimization algorithms, in: Proceedings of the 2017 Progress in Electromagnetics Research Symposium-Fall (PIERS-FALL), Singapore, 2017, pp. 832–837.
[47] J. Houseknecht, An ACO-Inspired, Probabilistic, Greedy Approach to the Drone Traveling Salesman Problem. Senior Honors Theses, 2019, pp. 849. https://digitalcommons.liberty.edu/cgi/viewcontent.cgi?article=1926&context=honors.
[48] Q. Dinh, D. Do, M. Hà, Ants can solve the parallel drone scheduling traveling salesman problem, in: GECCO '21: Proceedings of the Genetic and Evolutionary Computation Conference, 2021, pp. 14–21. https://doi.org/10.1145/3449639.3459342.
[49] R. Raj, C. Murray, The time-dependent multiple flying sidekicks traveling salesman problem: Parcel delivery with traffic congestion, 2021. https://ssrn.com/abstract=3767870.
[50] D.N. Das, R. Sewani, J. Wang, M.K. Tiwari, Synchronized truck and drone routing in package delivery logistics, IEEE Trans. Intell. Transp. Syst. 22 (9) (2021) 5772–5782.
[51] Q. Gu, T. Fan, F. Pan, C. Zhang, A vehicle-UAV operation scheme for instant delivery, Comput. Ind. Eng. 149 (2020), 106809.
[52] M. Dorigo, V. Maniezzo, A. Colorni, Ant system: optimization by a colony of cooperating agents, IEEE Trans. Syst. Man Cybern. Part B (Cybernetics) 26 (1) (1996) 29–41.
[53] M. Dorigo, L.M. Gambardella, Ant colony system: a cooperative learning approach to the traveling salesman problem, IEEE Trans. Evol. Comput. 1 (1) (1997) 53–66.